# Picosecond ultrasonic study of localized phonon surface modes in Al/Ag superlattices

Wei Chen,* Yu Lu, Humphrey J. Maris, and Gang Xiao
*Physics Department, Brown University, Providence, Rhode Island 02912*
(Received 17 June 1994)

We present the results of picosecond ultrasonic studies of localized acoustic-phonon surface modes in Al/Ag superlattices. By making measurements on a series of superlattices with different periods, we have been able to study surface modes with frequencies in the range from 110 to 670 GHz. The experiment reveals interesting variations in the surface-mode structure as the geometry of the cap layers is varied. We compare these results with the predictions of a transfer-matrix theory of the localized modes. The measured damping rate of the modes varies linearly with frequency and is nearly independent of temperature in the temperature range from 70 to 300 K. This variation of the attenuation with frequency and the order of magnitude of the attenuation are consistent with the assumption that the attenuation rises from an interaction between the phonon mode and the electrons, but the damping rate is about a factor of 5 larger than expected based upon Pippard's theory for bulk materials. It is likely that the enhancement in the damping rate is primarily due to losses occurring at the free surface of the structure.

## I. INTRODUCTION

Superlattice structures have interesting vibrational and transport properties that distinguish them from bulk materials.[1-3] Many of the differences in behavior are related to the folding of the dispersion relations for electrons and phonons that is associated with the periodicity of the superlattice structure. For phonons with a particular polarization, such folding normally gives rise to band gaps, i.e., frequency intervals in which no propagating phonon modes exist. The phonon spectrum and folding in superlattices have been studied by Raman-scattering studies,[4] and experiments using phonon transmission spectroscopy have demonstrated the existence of the band gaps.[5] Even though no propagating modes exist in the gaps, it is possible to have localized modes associated with the ends of the superlattice, or with other local disturbances from periodicity.[1,2]

In a previous paper[2] picosecond ultrasonic techniques have been used to study surface modes in a series of amorphous silicon-germanium multilayer structures with a range of bilayer thicknesses. For these samples it was possible to detect surface-mode oscillations at frequencies up to 124 GHz. In the multilayers with very short repeat distances, where the surface modes were expected to have high frequencies, no oscillations were detected. In this paper, we study surface modes of frequency up to 670 GHz in Al/Ag metallic superlattices. We have investigated the way in which the properties of the surface mode are modified by changes in the "capping" layers of the superlattice, i.e., by the geometry of the layers near to the free surface of the nanostructure. In addition, we have observed distinct damping of the surface modes. The damping rate was measured as a function of frequency and temperature. This damping may be due to a coupling between the vibration of the localized mode and the conduction electrons although, as we will discuss below, the damping rate is somewhat larger than expected.

## II. EXPERIMENTAL METHOD

### A. Picosecond ultrasonics

Picosecond ultrasonics has proven to be a useful technique for the study of the mechanical properties of thin films, superlattices, and other nanostructures.[6] In this type of experiment a subpicosecond light pulse is absorbed in some region of a nanostructure. The absorption of the light pulse sets up a local stress (see more detailed discussion below). The relaxation of this stress launches strain pulses that propagate through the structure. As these strain pulses propagate they change the optical properties of the different parts of the structure, and consequently lead to a change $\Delta R(t)$ in the overall optical reflectivity of the structure. This change is then measured by a probe pulse that is time delayed relative to the light pulse used to generate the phonons (the "pump" pulse).

The experimental configuration is shown schematically in Fig. 1. The pump and probe light pulses are focused onto an area of the structure that is approximately 20 $\mu$m in diameter. The light pulses used in the experiment were produced by a hybrid mode-locked dye laser operating at 6320 Å. For this wavelength the optical-absorption length is ~60 Å in bulk Al ~150 Å in bulk Ag. Thus even in the thinnest superlattices that we studied the light is absorbed in the first few layers of the structure.

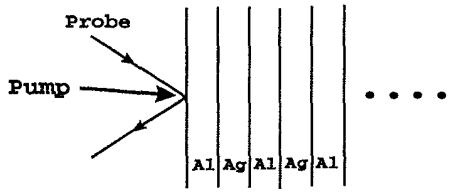


FIG. 1. Schematic diagram of the experiment.

 

There are two contributions to the stress that is produced by the absorbed light pulse. The energy of the light pulse is first given to the electrons in the metal. At this point the stress can be related to the change in the distribution function of the electrons. Let us suppose that the free surface of the superlattice lies in the $xy$ plane. For a free-electron gas the stress tensor $\sigma$ is isotropic, and at a depth $z$ into the superlattice its components are given by

$$\sigma_{\alpha\beta}(z) = -\tfrac{2}{3}\Delta E(z)\delta_{\alpha\beta} , \quad (1)$$

where $\Delta E(z)$ is the energy deposited per unit volume at a depth $z$ into the surface. Within a time on the order of a picosecond the electrons lose their energy to the lattice via the electron-phonon interaction. Because the lattice specific heat is much larger than that of the electrons (except at very low or very high temperatures) nearly all the energy is now in the lattice. Hence the components of the stress tensor are given by the formula

$$\sigma_{\alpha\beta}(z) = -\gamma_l \Delta E(z)\delta_{\alpha\beta} , \quad (2)$$

where $\gamma_l$ is the lattice Gruneisen constant. Generally, $\gamma_l$ is in the range 1–3, and so the lattice stress is somewhat larger than the electron stress. In addition to the complications arising from the two contributions to the stress, the generation mechanism is affected by the diffusion of the electrons that occurs before they lose their energy to the phonon bath.[7,8] As we will discuss below, this diffusion may have a substantial effect on the way in which the surface modes are excited.

Because the linear dimensions of the area that is excited by the pump pulse are much larger than the depth into the sample at which the energy is deposited, it is a good approximation to consider that the stress and the strain depend just on $z$, i.e., the motion is essentially one dimensional and perpendicular to the plane of the free surface. Therefore, the only surface modes studied by this technique are longitudinal modes with $k_x, k_y \approx 0$.

After the absorption of the light, the stress excites the vibrational modes of the superlattice structure. However, after a short time, the vibrations associated with the propagating modes will have moved deep into the superlattice and can no longer be detected by the probe pulse; only the motion associated with the localized surface modes remains near to the free surface. This component makes a contribution to the reflectivity change $\Delta R(t)$ which has the form of a persistent oscillation at a definite frequency. An example of this effect is shown in Fig. 2. These data were taken for a sample with 75 bilayers, each consisting of 121 Å of Al and 97 Å of Ag, and the layer that is adjacent to the free surface was an Al layer. Note the pronounced oscillations that persist beyond 190 psec. The frequency of the oscillations is 122 GHz.

In addition to the oscillatory component, $\Delta R(t)$ contains two other contributions. There is a smoothly decaying background which arises from the transient change in the temperature of the surface of the superlattice. For small $t$ (e.g., for $t < 20$ psec in Fig. 2), there is also a contribution from the propagating modes that are excited by the light pulse.

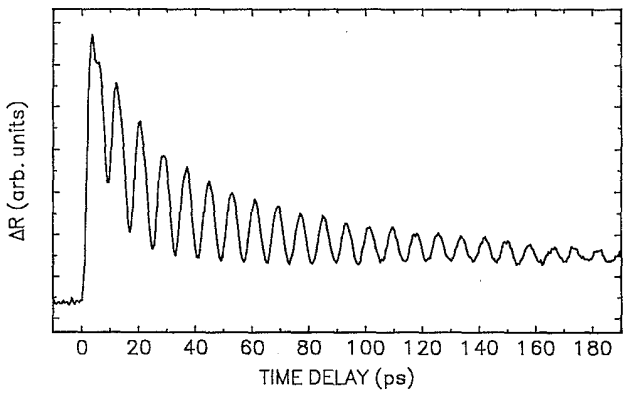


FIG. 2. Measured change $\Delta R(t)$ in optical reflectivity as a function of time. These data were taken for a sample with 75 layers, each consisting of 121 Å of Al and 97 Å of Ag.

In these experiments the pulse duration was 0.2 psec, the repetition rate was 76 MHz, and the energy of the light pulses used to generate the surface modes was 0.5 nJ. The amplitude of the oscillating strain was of the order of $10^{-6}$–$10^{-5}$. To improve the signal-to-noise ratio, we used lock-in techniques. The pump light was modulated at 1 MHz by an acousto-optic modulator.

### B. Sample growth and characterization

The superlattice samples used in this study were grown by using a high vacuum sputtering system equipped with three magnetron guns and a rotating substrate platform. The vacuum prior to sputtering was about $8 \times 10^{-8}$ Torr. During growth the Ar sputtering gas pressure was maintained at 4 mTorr. A buffer layer of Ag(111) about 400 Å in thickness was first grown on a Si(111) substrate at room temperature. Then alternating Al(111) and Ag(111) layers were deposited, followed by the growth of a cap layer. The deposition rates for both elements were kept at about 4 Å $\text{sec}^{-1}$. A computer controlled the movement of the substrate platform and the shutters above the individual guns. A series of samples were prepared with bilayer thicknesses ranging from 30 to 240 Å. The ratio $\gamma$ of the thickness of the Ag layers to the Al layers was approximately 0.8 in all of these samples. The total number of bilayers in each sample is about 70.

The structure of the samples has been analyzed with both low- and high-angle x-ray diffraction. Figure 3(a) shows a typical low-angle diffraction pattern characteristic of a periodic structure. We observe strong peaks up to high orders, which is indicative of the high regularity in the layered structure. The high-angle diffraction pattern of a sample is shown in Fig. 3(b). We have obtained layer and interface thicknesses for each sample by using a computer simulation program. It was assumed that inside the layers the composition as pure Al or Ag, and near the interface the composition was taken to vary linearly from pure Ag to Al over an interface thickness $\xi$. The solid curve in Fig. 3(a) is the result of a computer simulation based on assumed values for the layer thicknesses and the interface width, and is in reasonably

good agreement with the observed satellite diffraction pattern both as regards peak intensity and position. We found that the agreement between the simulation and the data is rather sensitive to the interface layer thickness. For all of our samples, $\xi$ falls into the range of 2.0–2.3 Å regardless of individual layer thickness. This value is of the order of a monolayer thickness, indicating that the interface in our samples is very sharp. The deduced layer thickness for each sample is consistent with the designed thickness during sample fabrication.

## III. THEORY OF SURFACE MODES

The calculation of the frequencies and displacement patterns associated with surface modes is most conveniently carried out using the transfer-matrix method.[1] We consider a superlattice (Fig. 4) consisting of alternating layers of materials 1 and 2 of thicknesses $d_1$ and $d_2$, densities $\rho_1$ and $\rho_2$, and sound velocities $v_1$ and $v_2$. The superlattice begins with $N$ capping layers that consist of alternating layers of materials 1 and 2 of thicknesses $d_1^{(i)}$ and $d_2^{(i)}(i=1,2,\ldots,N)$. The superlattice is taken to extend indefinitely in the positive-$z$ direction.

The equations of elasticity are

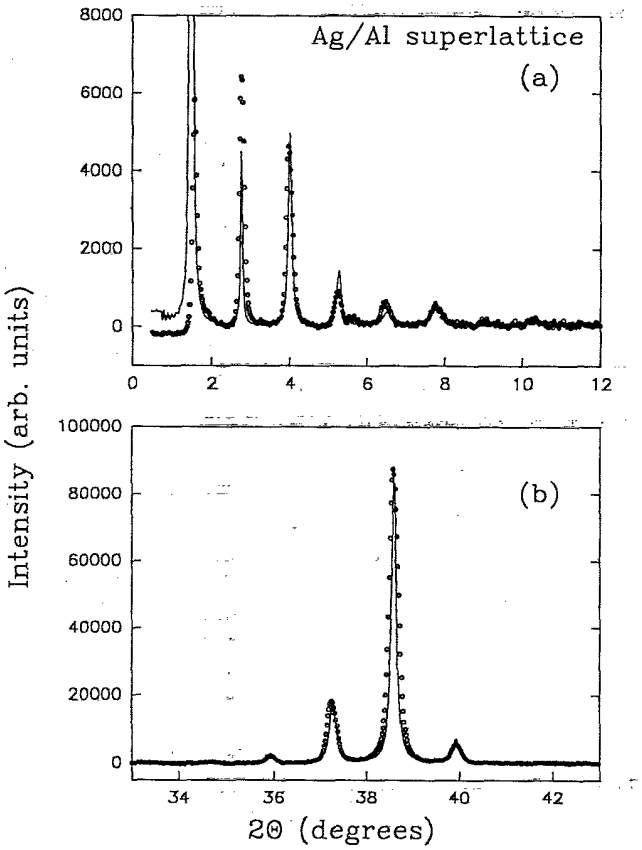


FIG. 3. Low-angle (a) and high-angle (b) x-ray-diffraction patterns from a Ag(111)/Al(111) superlattice. The solid curves show theoretical diffraction patterns calculated assuming an Ag layer thickness of 29 Å, an Al thickness of 41 Å, and an interface thickness of 2.3 Å.

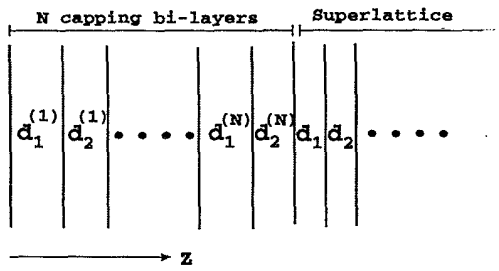


FIG. 4. Geometry of a superlattice with cap layers.

$$\rho\frac{\partial^2 u(z,t)}{\partial t^2}=\frac{\partial\sigma(z,t)}{\partial z}\ , \tag{3}$$

where $u$ is the displacement in the direction $z$, and $\sigma$ here denotes the $zz$ component of the stress tensor. This stress is related to the displacement by

$$\sigma(z,t)=\rho v^2\eta(z,t)\ , \tag{4}$$

where $\eta=\partial u/\partial z$ is the strain, and the values of the density $\rho$ and the sound velocity $v$ to be used depend on the particular layer.

We look for a solution in the form

$$u(z,t)=w(z)e^{-i\omega t}\ . \tag{5}$$

Let the $m$th bilayer of the superlattice begin at $z=z_m$. Then we can write the general solution of the wave equation in the part of this bilayer composed of material 1 as

$$w(z)=A_{m,1}\sin[k_1(z-z_m)]+B_{m,1}\cos[k_1(z-z_m)]\ , \tag{6}$$

and in layer 2 as

$$w(z)=A_{m,2}\sin[k_2(z-z_m-d_1)]+B_{m,2}\cos[k_2(z-z_m-d_1)]\ , \tag{7}$$

where $A_{m,1}$, $A_{m,2}$, $B_{m,1}$ and $B_{m,2}$ are constant amplitudes, and $k_1=\omega/v_1$ and $k_2=\omega/v_2$. At the interface between any two layers the displacement and the stress must be continuous. These conditions relate $A_{m,2}$ and $B_{m,2}$ to $A_{m,1}$ and $B_{m,1}$, $A_{m+1,1}$ and $B_{m+1,1}$ to $A_{m,2}$ and $B_{m,2}$, and so on. We can express these conditions in the form

$$\begin{bmatrix}A_{m+1,1}\\B_{m+1,1}\end{bmatrix}=T\begin{bmatrix}A_{m,1}\\B_{m,1}\end{bmatrix}\ , \tag{8}$$

defining $T$ as the transfer matrix of the superlattice. The elements of $T$ are

$$T_{11}=a_1a_2-p^{-1}b_1b_2\ , \tag{9}$$

$$T_{12}=-b_1a_2-p^{-1}a_1b_2\ , \tag{10}$$

$$T_{21}=b_1a_2+pa_1b_2\ , \tag{11}$$

$$T_{22}=a_1a_2-pb_1b_2\ , \tag{12}$$

where $a_1=\cos(k_1d_1)$, $a_2=\cos(k_2d_2)$, $b_1=\sin(k_1d_1)$, $b_2=\sin(k_2d_2)$, and $p=\rho_1v_1/\rho_2v_2$.

For a propagating mode in an infinite superlattice, it follows from Bloch's theorem that

$$\begin{bmatrix} A_{m+1,1} \\ B_{m+1,1} \end{bmatrix} = \lambda \begin{bmatrix} A_{m,1} \\ B_{m,1} \end{bmatrix} , \tag{13}$$

with $\lambda = e^{iqd}$, where $q$ is the wave number and $d$ is the bilayer thickness of the superlattice. Thus $\lambda$ must be an eigenvalue of $T$, so

$$\det|T - \lambda I| = 0 . \tag{14}$$

Hence we obtain the following dispersion relation for propagating modes:

$$\cos(qd) = \cos(\omega d_1/v_1)\cos(\omega d_2/v_2) - \frac{(1+p^2)}{2p}\sin(\omega d_1/v_1)\sin(\omega d_2/v_2) . \tag{15}$$

This determines $q$ for a given $\omega$. Once $\lambda$ is determined, the ratio of the amplitudes $A_{m,1}$ and $B_{m,1}$ can be found from Eqs. (8) and (13). The calculated dispersion curve for an Al/Ag superlattice, in which the thickness ratio $\gamma$ of Ag to Al is 0.8, is shown in Fig. 5. The parameters are taken to be the bulk values, i.e., $\rho_1 = 2.7$ g cm$^{-3}$, $\rho_2 = 10.5$ g cm$^{-3}$, $v_1 = 64$ Å psec$^{-1}$, and $v_2 = 40$ Å psec$^{-1}$. Note in Fig. 5 the existence of frequency band gaps, in which no propagating modes are allowed. In Fig. 5 the quantity plotted in the vertical direction is $\nu d$, where $\nu \equiv \omega/2\pi$.

We can also find surface-mode solutions that decrease in amplitude going into the superlattice. For these solutions Eqs. (8), (13), and (14) still hold, but now it is necessary that $|\lambda| < 1$. The frequency of the mode and the value of $\lambda$ are determined by the requirement that the stress be zero at the free surface of the structure. To solve this problem it is convenient to define transfer matrices for the cap layers. For the $n$th cap bilayer we define the transfer matrix $T_c^{(n)}$ by

$$\begin{bmatrix} A_{c,1}^{(n+1)} \\ B_{c,1}^{(n+1)} \end{bmatrix} = T_c^{(n)} \begin{bmatrix} A_{c,1}^{(n)} \\ B_{c,1}^{(n)} \end{bmatrix} , \tag{16}$$

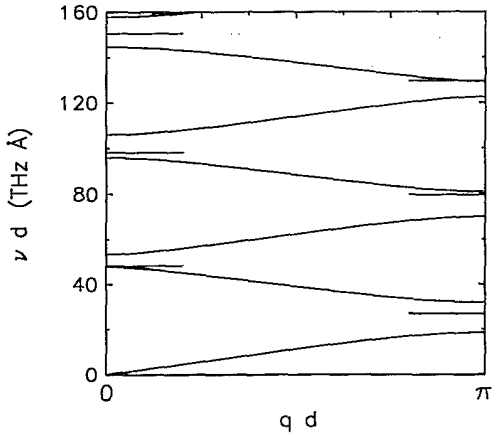


FIG. 5. Dispersion relation for longitudinal acoustic waves propagating through an Al/Ag superlattice. $\nu$ is the frequency, $q$ is the wave number, and $d$ is the bilayer thickness. These results are based on the use of the elastic properties of bulk Al and Ag. The horizontal bars indicate the frequencies of the localized surface modes that exist in the structure when it is terminated with an Al layer.

where $A_{c,1}^{(n)}$ and $B_{c,1}^{(n)}$ are the amplitudes in layer 1 of the $n$th cap bilayer. The elements of $T_c^{(n)}$ are given by equations analogous to Eqs. (9)–(12), allowing for possibly different thicknesses of the individual layers. We can then define a matrix $T_c$ which relates the amplitudes $A_{c,1}^{(1)}, B_{c,1}^{(1)}$ in the first cap layer to the amplitudes $A_{1,1}, B_{1,1}$ in the first layer of the main part of the superlattice. Thus

$$\begin{bmatrix} A_{1,1} \\ B_{1,1} \end{bmatrix} = T_c \begin{bmatrix} A_{c,1}^{(1)} \\ B_{c,1}^{(1)} \end{bmatrix} . \tag{17}$$

It follows that

$$T_c = T_c^{(N)} T_c^{(N-1)} \cdots T_c^{(2)} T_c^{(1)} . \tag{18}$$

The condition that the stress be zero at the free surface of the superlattice requires that $A_{c,1}^{(1)}$ be zero. Therefore, from Eq. (17), we have

$$\frac{A_{1,1}}{B_{1,1}} = \frac{T_{c,12}}{T_{c,22}} \equiv C . \tag{19}$$

Substituting into Eqs. (8) and (13), we arrive at the final equations for determining the eigenfrequencies and mode patterns of the surface modes:

$$T_{21}C^2 + (T_{22} - T_{11})C - T_{12} = 0 , \tag{20}$$

$$\lambda = T_{21}C + T_{22} , \tag{21}$$

where $|\lambda|$ must be less than 1 so that the localized mode decreases in amplitude with distance $z$ into the superlattice. The exponential decay length $l$ for the surface mode is given by

$$l = d/|\ln(|\lambda|)| . \tag{22}$$

These general results can readily be incorporated into a computer program to calculate the normal modes of a superlattice with arbitrary cap layers. In the following, we apply the results to several special cases.

(a) A *regular* superlattice with no cap bilayer. We can simply set $N = 0$ and so $T_c$ is the unit matrix. Thus from Eq. (19), $C = 0$. From Eq. (20) we have $T_{12} = 0$, which gives

$$p\tan(\omega d_1/v_1) + \tan(\omega d_2/v_2) = 0 . \tag{23}$$

This relation gives the frequency of a possible surface mode. From Eq. (21) we obtain

$$\lambda = \frac{\cos(\omega d_1/v_1)}{\cos(\omega d_2/v_2)} . \tag{24}$$

In order for this to be a localized surface mode it is necessary that $|\lambda| < 1$. This formula has been derived previously.[2]

(b) A regular superlattice plus a single cap layer of material 2 of thickness $d_c$. We now take $N = 1$ and $d_{c,1}^{(1)} = 0$ and $d_{c,2}^{(2)} = d_c$. Therefore, $C = -p^{-1}\tan(k_2 d_c)$. Substituting into Eq. (20), we have

$$\tan\phi_2+p\tan\phi_1\left[\cos^2\phi_c+p^{-2}\sin^2\phi_c-\frac{1-p^2}{p^2}\tan\phi_2\sin\phi_c\cos\phi_c\right]=0\ . \quad (25)$$

From Eq. (21), the eigenvalue is

$$\lambda=\cos\phi_1\cos\phi_2-p\sin\phi_1\sin\phi_2-p^{-1}\tan\phi_c(\sin\phi_1\cos\phi_2+p\cos\phi_1\sin\phi_2)\ , \quad (26)$$

where $\phi_1=\omega d_1/v_1$, $\phi_2=\omega d_2/v_2$, and $\phi_c=\omega d_c/v_2$. For the localized surface mode, it is again necessary that $|\lambda|<1$.

(C) A regular superlattice plus a single cap bilayer with thicknesses of the layers of material 1 and 2 equal to $d_{c1}$ and $d_{c2}$, respectively. Proceeding in the same way as above, we then obtain

$$C=\frac{-\sin\phi_{c1}\cos\phi_{c2}-p^{-1}\cos\phi_{c1}\sin\phi_{c2}}{\cos\phi_{c1}\cos\phi_{c2}-p\sin\phi_{c1}\sin\phi_{c2}}\ , \quad (27)$$

where $\phi_{c1}=\omega d_{c1}/v_1$, $\phi_{c2}=\omega d_{c2}/v_2$. The frequency and value of $\lambda$ can then be calculated from Eqs. (20) and (21).

## IV. EXPERIMENTAL RESULTS AND DISCUSSION

### A. Regular superlattices: zone-boundary surface modes

We have studied a series of regular superlattices in which the ratio $\gamma$ of the Ag-to-Al thickness was 0.8. The repeat distance of the structure varied from 50 to 227 Å. The layer adjacent to the free surface in each of these samples is Al. For the superlattices of repeat distance $d$ down to 70.4 Å, a persistent oscillation was present that was clearly related to a localized surface mode (see, for example, Fig. 2). For each sample only one such persistent oscillation frequency could be detected. When samples with smaller repeat distances were investigated, no such oscillation could be detected. The results for the surface-mode frequencies are listed in Table I. The highest frequency of the zone-boundary surface mode that we were able to detect is 303 GHz. The uncertainties in the measured frequencies are typically less than 1%.

To compare these results with theory, we used Eqs. (23) and (24) to find theoretical surface-mode frequencies. The results are included in Fig. 5. A series of surface modes are found both at the zone-boundary and zone-center phonon band gaps. The numerical values of the frequency of the surface mode in the first zone-boundary energy gap for the particular layer thicknesses that we studied are listed in Table I. Since the frequency of this mode is within 20% of the experimentally measured frequencies, it is clear that this must be the mode that is detected in the experiment. The theoretical $\nu_{th}$ and experimental $\nu_{exp}$ frequencies agree to within a few percent for the superlattices with large repeat distances, but differ by an increasing amount as the period becomes smaller. When the repeat distance is 70.4 Å, $\nu_{exp}$ is 20% less than $\nu_{th}$.

We now consider some possible origins of this discrepancy. The bilayer thickness of the superlattices is known with an accuracy believed to be better than 1.4%, and so the uncertainty in $\nu_{th}$ arising from this is much too small to explain the discrepancy. A second possibility is that the elastic properties of the material composing the superlattice could be different from the bulk values. There have been a number of reports in the literature of anomalous elastic properties of thin films.[9] However, most of these experiments have been studies of thinner layers than those involved here and, in addition, have given indications that the elastic moduli are *increased* for thin films. We performed a separate experiment to look for a change in the sound velocity, and the results are shown in Fig. 6. The sample is a superlattice of period $d=106$ Å with an Ag cap layer, and measurements of the change $\Delta R(t)$ in the optical reflectivity have been made out to 900 psec. Two echoes are visible (the second is weak). These echoes arise from strain waves which have been generated at the free surface of the superlattice, propagated through to the substrate, and then been reflected back to the free surface. From the arrival time of the echo and the known thickness of the structure, we obtain a sound velocity of $51\pm2$ Å psec$^{-1}$. To within the experimental error, measurements on samples with other bi-

TABLE I. Comparison of the experimentally measured surface-mode frequencies ($\nu_{exp}$) with those calculated from the transfer-matrix theory: $\nu_{th}$ (without taking into account the Al oxidation) and $\nu_{Ox}$ (taking into account the oxidation).

| Bilayer thickness (Å) | $\nu_{th}$ (GHz) | $\nu_{exp}$ (GHz) | $\nu_{Ox}$ (GHz) |
|---|---|---|---|
| 227 | 117 | 110 | 109 |
| 218 | 122 | 122 | 113 |
| 163 | 166 | 151 | 153 |
| 120 | 222 | 196 | 199 |
| 89.3 | 298 | 251 | 265 |
| 70.4 | 376 | 303 | 334 |

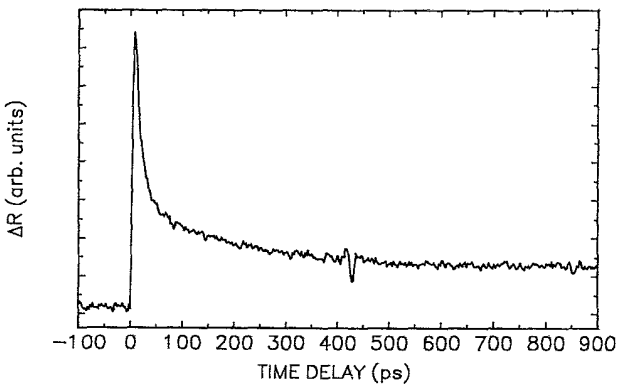


FIG. 6. Experiment to measure the average sound velocity in a superlattice. The measured change $\Delta R(t)$ in optical reflectivity is shown as a function of time. The echo at 420 psec originates from a strain pulse that has propagated through the entire superlattice, been reflected at the interface to the substrate, and then returned to the free surface.

layer thicknesses give the same result. This compares with a velocity calculated from the macroscopic elastic constants and densities of Al and Ag of 50.7 Å psec$^{-1}$. Thus this experiment gives no clear evidence for a significant modification of the elastic properties in thin films.

It appears more likely that the details of the cap layer play a significant role. Let us suppose, for example, that the structure as prepared by sputtering is geometrically perfect. After removal from the sputtering system, the surface of the first Al layer will oxidize. Let us suppose that an oxide layer is formed that has a thickness $d_{\mathrm{Ox}}$ and density $\rho_{\mathrm{Ox}}$, and that the thickness of the Al layer becomes $d'_{\mathrm{Al}}$. Then, taking the oxide to have the composition $Al_2O_3$, we find

$$d'_{\mathrm{Al}}=d_1-0.53\frac{\rho_{\mathrm{Ox}}d_{\mathrm{Ox}}}{\rho_{\mathrm{Al}}}, \tag{28}$$

where $d_1$ is the starting thickness of the Al layer. If we use the density of bulk crystalline $Al_2O_3$, this gives the relation $d'_{\mathrm{Al}}=d_1-0.78d_{\mathrm{Ox}}$. Using this relation and the theory in Sec. III, we have calculated the zone-boundary surface-mode frequency as a function of the thickness percentage of the Al cap layer that is oxidized. The result is shown in Fig. 7, where $\nu_0$ is the frequency of surface mode assuming no oxidation. Clearly, the surface-mode frequency decreases with increasing thickness of oxidized layer up to about 45%. For aluminum that has been oxidized by exposure to the atmosphere at room temperature, the thickness of the oxidized layer is typically 25–30 Å.[10] The surface-mode frequencies $\nu_{\mathrm{Ox}}$ that we calculated by taking into account this oxidized layer (assumed thickness of 25 Å) are listed in Table I. They are in much better agreement with the experimental data than those calculated assuming no oxidation. The discrepancies that remain may, at least in part, be attributed to the uncertainty in the ratio $\gamma$ of the Ag-to-Al layer thickness.

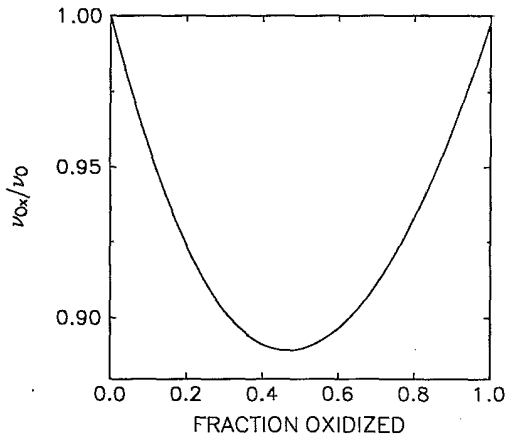


FIG. 7. Effect of the oxidation of the Al cap layer on the surface-mode frequency ($\nu$). The horizontal axis is the fraction of the thickness of the Al cap layer that has oxidized. The calculation is done for the lowest zone-boundary surface mode in a regular superlattice with $\gamma=0.8$.

Finally, we consider why it is that below a critical repeat distance of the superlattice no zone-boundary surface-mode oscillations can be see, or equivalently why they can only be seen up to a certain frequency. This is not a result of the finite duration of the pump and probe light pulses, since the hybrid mode-locked laser provides us with a laser-pulse duration less than 0.2 psec, and in previous experiments we have generated and detected vibrations with frequencies up to 440 GHz with the same apparatus. A second possibility is that it comes about because of the time it takes the stress to be set up in the structure. As we discussed in Sec. II, there is an electronic contribution to the stress that appears immediately after the light is absorbed, and a lattice contribution that appears at a time $\tau$ of the order of 1 psec later.[8] The lattice contribution is expected to be larger. Thus, for samples in which the surface mode frequency is sufficiently low, the lattice stress could make a significant contribution to the generation process, whereas in thinner samples only the electronic stress would have time to act. The crossover should occur at the frequency $\nu$ such that

$$2\pi\nu\tau\approx 1, \tag{29}$$

and so if $\tau=1$ psec, $\nu=160$ GHz. Thus this mechanism could give a reduction in amplitude of the surface mode as the frequency increases, possibly causing the signal to drop below the noise level at some frequency. A third factor to consider is the degree to which the stress pattern set up when the light is absorbed matches the vibrational pattern of the surface mode. For a very short-period superlattice the light absorption occurs over several repeat distances, and so the stress pattern will have approximately the periodicity of the lattice. This will couple very poorly to a *zone-boundary* surface mode whose amplitude changes sign from one bilayer to the next.[2] This effect will be enhanced by the very rapid diffusion of the hot electrons excited by the light pulse;[8] thus even if the light itself is absorbed in the first bilayer or so, the electrons may well diffuse through several layers before they lose their energy to the lattice.

### B. Effect of cap layers on surface modes

Based upon the results just described, it is clear that the localized surface modes are very sensitive to the cap-layer geometry and thickness. We have used the transfer-matrix theory to calculate the modes for superlattices with a variety of different cap layers. One interesting result is that for some geometries one can obtain more than one surface mode in a single frequency gap. As an example, consider a superlattice in which there are two capping bilayers, each with a thickness $d_{\mathrm{cap}}$ that is varied. The thickness ratio of Ag to Al in the cap layers is taken to be the same as that inside the superlattice. For this structure the frequencies of surface modes lying within the lowest zone-boundary gap are shown in Fig. 8. These calculations are for a repeat distance of 210 Å. This type of structure may have several localized surface modes lying within the same gap. When $d_{\mathrm{cap}}=1.2d$, for example, there are two surface modes with frequencies 106 and 148 GHz. The calculated strain profiles of the

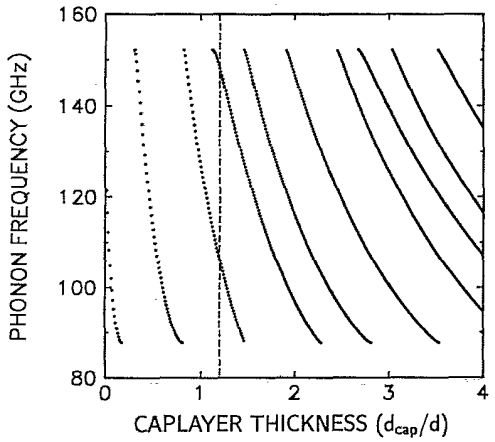


FIG. 8. Frequency of the zone-boundary surface modes in an Al/Ag superlattice with $d=210$ Å and $\gamma=0.8$ and two double cap layers as a function of the capping bilayer thickness $d_{cap}$. $d$ is the repeat distance of the periodic part of the structure. The dashed line indicates the position of $d_{cap}=1.2d$.

two modes are as shown in Fig. 9. We fabricated a sample with this geometry, and the results of measurements on this sample are shown in Fig. 10. Beating between the two surface modes is clearly seen. The experimentally measured frequencies are 100 and 144 GHz, and are thus in good agreement with the theory. (We mention in passing that beating and coherent oscillations of optical-phonon modes have been studied in Ref. 11.)

We have also investigated the effect of an Ag cap layer. It is straightforward to show that if there is a single Ag

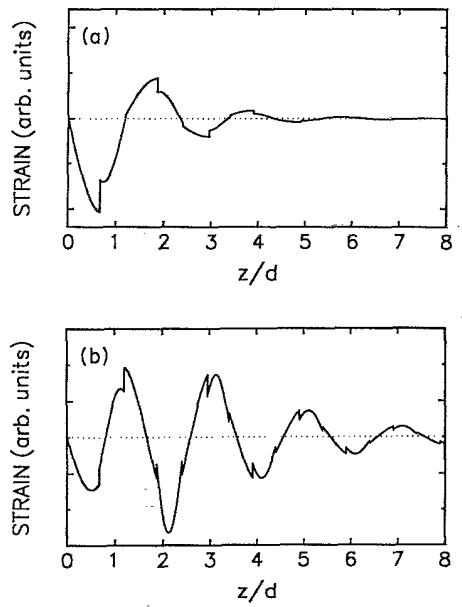


FIG. 9. Calculated strain profiles of the two localized surface modes for the double cap-layer structure described in the text: (a) for the mode of 106 GHz, and (b) for 148 GHz. $z$ is the distance into the structure, and $d$ the repeat distance of the periodic part of the structure.

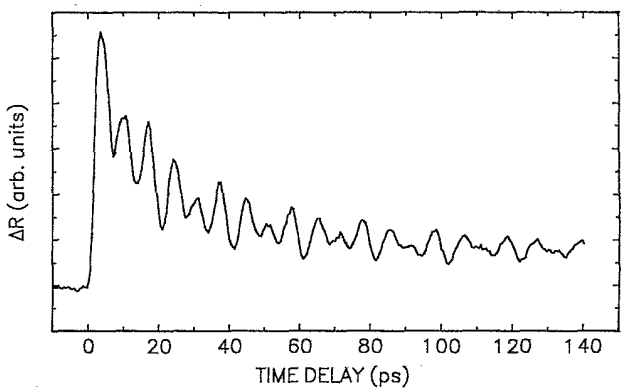


FIG. 10. Measurement of the change $\Delta R(t)$ in optical reflectivity as a function of time for the double cap-layer structure described in the text. The response consists of weakly damped oscillation at 100 and 144 GHz.

cap layer of thickness $d_{cap}$ equal to the thickness $d_2$ of the Ag layers in the periodic part of the structure, there cannot be any surface modes.[2] We have investigated several samples of this type and have seen no surface modes (e.g., no surface-mode oscillation is seen in Fig. 6). For several samples with a single Ag cap layer of thickness $d_{cap}$ not equal to $d_2$, we have been able to detect surface modes. It is interesting that in these samples no zone-boundary surface mode was detected, but instead a zone-center surface mode whose frequency is about twice that of the zone-boundary gap. As an example, in Fig. 11 we show data obtained from a superlattice of bilayer thickness $d=106$ Å. The oscillation frequency is 480 GHz, and this mode lies in the lowest zone-center phonon band gap.

To explain the above observation, we use Eqs. (25) and (26) and vary the Ag cap-layer thickness while looking for surface-mode frequencies that lie in either the zone-boundary or zone-center band gaps. The results are shown in Fig. 12. Note that when $0.95d_2 > d > 0.5d_2$, no zone-boundary surface-mode solution exists, but there is a zone-center-mode solution. This is consistent with the experimental results above. To have a frequency of the

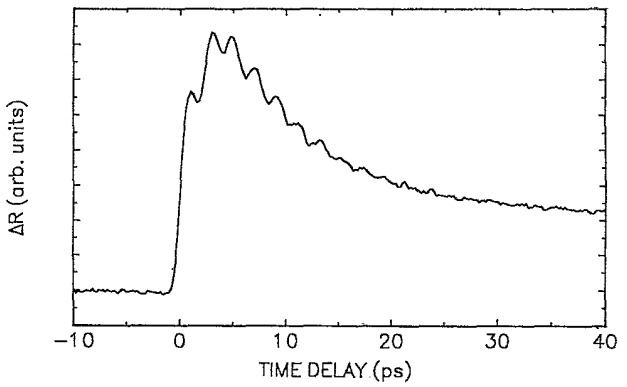


FIG. 11. Measurement of the change $\Delta R(t)$ in optical reflectivity for a superlattice with an Ag cap layer. The frequency of the oscillations is 480 GHz.

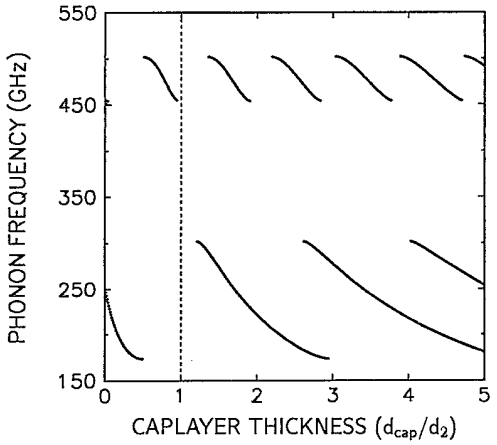


FIG. 12. Effect of the Ag cap-layer thickness on the surface-mode structure, calculated for a superlattice of $d=106$ Å and $\gamma=0.8$. Note that no surface mode exists when $d_{cap}=d_2$ (the dashed line).

zone-center mode of 480 GHz, the Ag cap layer should be about $0.75d_2$.

We have looked at a number of other samples with this geometry. The highest-frequency zone-center mode that we have been able to detect had a frequency of 670 GHz, and was excited in a sample with 80-Å repeat distance.

### C. Damping of surface modes

To investigate the damping of the surface modes, we took the results of a measurement of $\Delta R(t)$, as shown in Fig. 2, and subtracted the smoothly varying background term arising from thermoreflectance.[12] The remaining contribution could be fit very well by an exponentially damped oscillation. The measured damping rate $\Gamma$ for surface modes in a number of superlattices at room temperature are plotted as a function of the mode frequency in Fig. 13(a). For the zone-boundary modes the damping is found to be approximately proportional to frequency. An accurate measurement for a zone-center mode could be made only at a single frequency (480 GHz). The damping of this mode is about a factor of 2 higher than would be expected on the basis of an extrapolation of the lower-frequency data for the zone-boundary modes. The damping is almost independent of temperature in the range down to 70 K; this is shown in Fig. 13(b).

At first sight the linear variation of the damping with frequency suggests that the damping may be due to the electron-phonon interaction. In a bulk metal the damping rate of a longitudinal sound wave is given by Pippard's formula[13]

$$\alpha=\frac{nm}{2\rho\tau}\left[\frac{q^2\Lambda^2\tan^{-1}q\Lambda}{3(q\Lambda-\tan^{-1}q\Lambda)}-1\right], \tag{30}$$

where $n$ is the number density of free electrons, $m$ the electron mass, $\tau$ the electron-scattering time, $\Lambda$ the electron mean free path, and $q$ the wave number of the sound wave. Equation (30) gives the rate of attenuation of the sound amplitude per unit time. It has the following limiting forms:

$$\alpha=\frac{\pi^2 nmv_F\nu}{6\rho v}, \quad q\Lambda\gg 1, \tag{31}$$

$$\alpha=\frac{4\pi nmv_F\nu}{15\rho v}q\Lambda, \quad q\Lambda\ll 1, \tag{32}$$

where $\nu$ is the sound frequency, $v_F$ the Fermi velocity, and $v$ the sound speed. Based on estimates of $\Lambda$ from electrical resistance measurements we have made on the samples at room temperature, we find that $q\Lambda$ is comparable to or somewhat larger than 1 for frequencies in our measurement range. Hence as a rough approximation we can take the attenuation to be given by Eq. (31), i.e., to be proportional to frequency and independent of temperature. This is the behavior that we have found in our experiments.

However, there are a number of difficulties with this interpretation. The first is that the damping rate is too small. In Fig. 13(a) we include the predictions of Eq. (31)

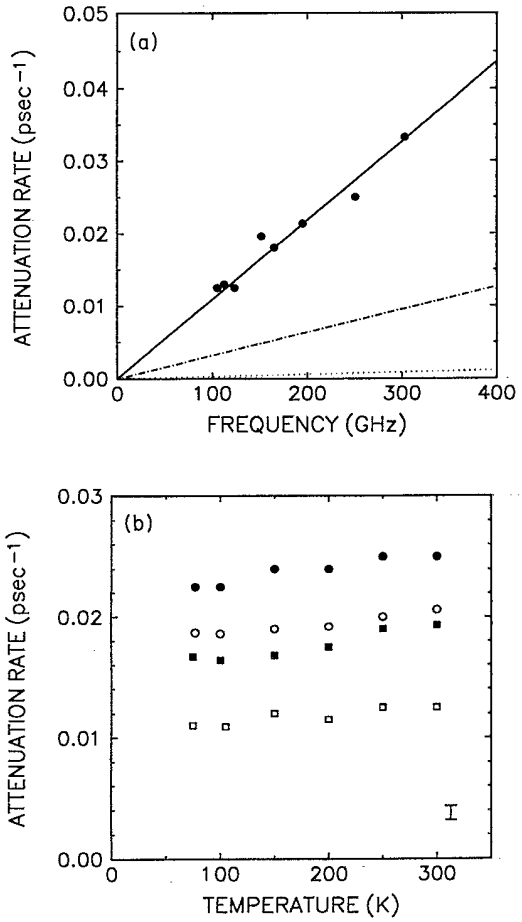


FIG. 13. Measured damping rate for the zone-boundary surface modes in regular superlattices. (a) shows the damping as a function of frequency. The straight solid line is a least-squares fit to the zone-boundary mode data, and the dotted and dashed lines are plots of the Pippard formula [Eq. (30)] for bulk Al and Ag, respectively. (b) shows the damping as a function of temperature (● for the sample of $d=89.3$ Å; ○ for $d=120$ Å; filled boxes for $d=163$ Å; and empty boxes for $d=227$ Å). Vertical bar indicates the uncertainty in the results.

for longitudinal waves in bulk Al and Ag. The result for Al is about three times smaller than the experimental values, and for Ag the difference is approximately a factor of 24. If $q\Lambda$ were less than 1 the theoretical attenuation would be reduced even further. Previous studies on bulk Al (Refs. 14 and 15) have shown that the band structure of bulk Al can alter the Pippard's attenuation result, but the change is typically less than 20%, and is much too small to explain the observed enhancement.

Of course, the Pippard formula gives the attenuation of sound by free electrons in bulk metals, and so one can propose that the attenuation we have measured is increased because of the effects of the band structure of the superlattice.[16] We have not attempted to construct a detailed theory of this type of correction to the Pippard formula. However, we have performed some simple experiments that suggest that the measured attenuation may not in fact arise from the electron-phonon interaction. We note that according to the Pippard formula the damping rate in Al is about a factor of 10 larger than in Ag. Thus, if electrons are the source of the damping, one would expect a larger damping in superlattices that contain a larger volume of Al than Ag. To test this idea we prepared samples in which the Al thickness ($d_1$) was not equal to the silver thickness ($d_2$). The characteristics of three such samples are listed in Table II. The damping of a sound wave is associated with the coupling of the strain field of the wave with the conduction electrons. Thus one expects that, as a first approximation, superlattices in which the oscillating strain is primarily in the Al should have a much larger damping rate than those in which it is in the Ag. For each sample we calculated the vibration pattern of the zone-boundary surface mode, and then evaluated the fraction of the strain energy that was in the Al part of the structure (see Table II). For the three samples studied this fraction varied from 10 to 76%. However, there was no significant change in the damping rate, thus suggesting that electrons are not the source of the damping.

Given this result, what can be the origin of the damping? The differences in thermal properties of the Al and Ag will lead to differences in temperature between adjacent layers, and these temperature differences will lead to heat flow across the interfaces and dissipation. The flow of heat will be limited in part by the Kapitza resistance at the interfaces. This process is similar to the well-known Zener damping in polycrystalline metals. We have estimated the damping due to this effect, and find that it is at least one order of magnitude smaller than the experimental results. It also appears that the attenuation due to phonon-phonon interactions is too small and does not depend on frequency and temperature in the required way, provided that there is no substantial modification of the phonon-phonon interaction due to the superlattice structure. As far as we can see, the most likely source of the damping is some process that occurs at the free surface of the structure. There is an extensive literature concerning the scattering and absorption of phonons at surfaces.[17] To relate to this body of work, we note the following. Qualitatively, we can consider that the surface mode is a wave that travels into the structure a distance on the order of the exponential decay length $l$ [see Eq. (22)], and then returns to be reflected from the free surface of the structure. Thus in unit time the wave undergoes on the order of $v/2l$ reflections at the free surface. Let us suppose that there is some effect that causes this reflection coefficient $r$ to be less than 1. Then the attenuation of the surface mode per unit time would be

$$\alpha=(1-r)\frac{v}{2l} . \tag{33}$$

Since $l$ varies as $\nu^{-1}$, this gives a damping proportional to frequency if $r$ is taken to be frequency independent in the sub-THz frequency range. To cause the magnitude of the damping to agree with experiment we would need to have

$$1-r\approx 0.06 . \tag{34}$$

The previous experimental measurements of $(1-r)$ referred to above are from low-temperature experiments but with sound waves (phonons) in the same frequency range as studied here. A wide range of values for $(1-r)$ has been obtained, dependent on the material studied and the condition of the surface, and the origin of the loss at the surface is still not understood. However, these experiments certainly show that a reflection loss at least as large as 6% can occur.

TABLE II. Samples used to investigate the damping of surface modes by the electron-phonon interaction.

| Sample | Al thickness (Å) | Ag thickness (Å) | Strain energy in Al (%) | Damping rate per cycle |
|---|---|---|---|---|
| *A* | 70 | 130 | 10 | 0.10 |
| *B* | 100 | 100 | 43 | 0.10 |
| *C* | 130 | 70 | 76 | 0.11 |

## ACKNOWLEDGMENTS

We would like to thank S. Das Sarma, L. B. Freund, A. V. Nurmikko, and A. Zheleznyak for helpful discussions. This work was supported in part by the U.S. National Science Foundation through the Materials Research Program at Brown University, Grant No. DMR-9121747.

*Present address: IBM Thomas J. Watson Research Center, P.O. Box 218, Yorktown Heights, NY 10598.

[1]B. Djafari-Rouhani, L. Dobrzyanski, O. Hardouin Duparc, R. E. Camley, and A. A. Maradudin, Phys. Rev. B **28**, 1711 (1983); R. E. Camley, B. Djafari-Rouhani, L. Dobrzynski, and A. A. Maradudin, *ibid.* **27**, 7318 (1983).

[2]H. T. Grahn, H. J. Maris, and J. Tauc, Phys. Rev. B **38**, 6066 (1988).

[3]S. Tamura, D. C. Hurley, and J. P. Wolfe, Phys. Rev. B **38**, 1427 (1988); S. Tamura, *ibid.* **39**, 1261 (1988).

[4]C. Colvard, R. Merlin, M. V. Klein, and A. C. Gossard, Phys. Rev. Lett. **45**, 298 (1980).

[5]V. Narayanamurti, H. L. Stormer, M. A. Chin, A. C. Gossard, and W. Wiegmann, Phys. Rev. Lett. **43**, 2012 (1979).

[6]H. T. Grahn, H. J. Maris, and J. Tauc, IEEE J. Quantum Electron. **QE-25**, 2562 (1989).

[7]R. W. Schoenlein, W. Z. Lin, and J. G. Fujimoto, and G. L. Eesley, Phys. Rev. Lett. **58**, 1680 (1987); H. E. Elsayed-Ali, T. B. Norris, M. A. Pessot, and G. A. Mourou, *ibid.* **58**, 1212 (1987).

[8]G. Tas and H. J. Maris, Phys. Rev. B **49**, 15 046 (1994).

[9]See, for example, A. Fartash, E. E. Fullerton, I. K. Schuller, S. E. Bobbin *et al.*, Phys. Rev. B **44**, 13 760 (1991).

[10]S. Wernick, R. Pinner, and P. G. Sheasby, in *The Surface Treatment and Finishing of Aluminium and Its Alloys* (ASM International, Metals Park, OH, 1985), Vol. 1, p. 5.

[11]W. A. Kütt, W. Albrecht, and H. Kurz, IEEE J. Quantum Electron. **QE-28**, 2434 (1992).

[12]H. N. Lin, R. J. Stoner, H. J. Maris, and J. Tauc, J. Appl. Phys. **69**, 3816 (1991); W. Chen, H. J. Maris, Z. R. Wasilewski, and S. Tamura (unpublished).

[13]A. B. Pippard, Proc. R. Soc. London, Ser. A **257**, 165 (1960); Philos. Mag. **46**, 388 (1955); **46**, 1104 (1955).

[14]K. C. Hepfer and J. A. Rayne, Phys. Rev. B **4**, 1050 (1971).

[15]J. A. Rayne, C. K. Jones, in *Physical Acoustics,* edited by W. P. Mason and R. N. Thurston (Academic, New York, 1970), Vol. 7, p. 149.

[16]B. Y. Jin and J. B. Ketterson, Adv. Phys. **38**, 189 (1989).

[17]See, for example, R. O. Pohl and B. Stritzker, Phys. Rev. B **25**, 3608 (1982); T. Klitsner and R. O. Pohl, in *Phonon Scattering in Condensed Matter V,* edited by A. C. Anderson and J. P. Wolfe (Springer, Berlin, 1986), p. 162.